Dynamics of scroll waves in a cylinder jacket geometry

Christian Bruns,* and Marcus J. B. Hauser†
Institut für Experimentelle Physik, Abteilung Biophysik, Otto-von-Guericke Universität Magdeburg, Universitätsplatz 2, 39106 Magdeburg, Germany
and Institut für Biometrie und Medizinische Informatik, Otto-von-Guericke Universität Magdeburg, Leipziger Strasse 44, 39120 Magdeburg, Germany
(Received 12 April 2017; published 5 July 2017)

The dynamics of scroll waves in a narrow cylinder jacket–shaped reactor is investigated experimentally by optical tomography. The fate of the scroll waves of excitation in the Belousov-Zhabotinsky reaction depends on the thickness of the cylinder jacket. While at sufficiently wide cylinder jackets vertically oriented scroll waves remain stable, the probability that the filament of a scroll hits a lateral wall increases as the cylinder jacket narrows. This may lead to the rupture of the initial filament and pinning of the filament ends at the lateral walls. Filaments that pin to opposite lateral walls shrink and reorient to a horizontal orientation; such a reorientation corresponds to a transition from an intramural to a transmural scroll wave. The kinetics of the reorientation and shrinkage of the scrolls were studied. Furthermore, we find that no new filaments were generated upon collision of excitation waves at the side of the cylinder jacket opposite to the scroll wave. Thus, under the studied conditions, we do not observe any new generation of filaments due to a phenomenon like reentry.

DOI: 10.1103/PhysRevE.96.012203

I. INTRODUCTION

Excitable media are frequent in biological systems but they also occur in physical and chemical systems. In biology, excitable media are found at the level of tissues and organs, as, for instance, in certain types of cardiac arrhythmias [1,2], the coherent contraction of the uterus during labor [3], the grey matter in the brain's visual cortex [4,5], as well as on the cellular level, as in fused cells of the amoeba *Dictyostelium discoideum* [6]. Most biological excitable systems (like organs and tissues) are rather three-dimensional (3D) than two-dimensional (2D) objects; therefore, the 3D nature of such excitable systems needs to be taken into account.

Scroll waves of electric excitation are at the basis of some cardiac arrhythmias, for instance ventricular tachycardia [1,2]. During ventricular tachycardia the scroll wave may lose its stability and break up into two or more scroll waves. This leads to ventricular fibrillation [2,7–9] which, due to its severity, has sparked numerous simulation studies of scroll wave dynamics in the context of cardiac arrhythmias (see Refs. [10,11] and references therein).

Experimental studies of excitation waves and their dynamics remain challenging, especially because of the difficulties in visualizing such waves of electrical activity in usually opaque tissues and organs. To obtain a better understanding, two approaches have been adopted, namely, extensive numerical simulations and the study of experimental model systems. The latter are excitable systems that are transparent and whose excited states are optically distinct from the respective resting (quiescent) states. These properties allow for a monitoring of the excitability in the experimental model by optical tomography [12,13]. One prominent example is the Belousov-Zhabotinsky (BZ) reaction, which has frequently been used for detailed experimental studies of the dynamics of 3D excitable systems [13–21].

In the heart the dynamics of excitation waves is a result of a multitude of interacting factors that lead to a complex situation, where the excitable dynamics is coupled to the complex geometry of the organ, which on top changes due to the chemomechanical coupling caused by the heart beat. In addition, the tissue is not homogeneous and displays a preferential orientation for the propagation of excitation waves due the anisotropic nature of the fibers in the muscle.

To gain insights into the contribution of the individual factors, the dynamics and evolution of scroll waves and rings in model systems is frequently studied under idealized conditions, i.e., in homogeneous and isotropic media of simple geometry. Typical patterns observed in 3D excitable systems are traveling waves and scroll waves. The latter are the 3D counterparts of spiral waves observed in two-dimensional systems and they rotate around a line defect, the so-called filament [15,22,23]. When the filament forms a closed line, the corresponding excitation wave is called a scroll ring.

The dynamics of scroll waves as well as the instabilities leading to changes in shape and properties of the filaments have attracted considerable interest. In homogeneous media, scroll waves may be destabilized by several instabilities, for instance, when the line tension of their filaments becomes negative [15,24–26] or through a 3D meandering instability [15,27,28].

In a gradient field, scroll waves may also suffer a twist-induced instability that is also called "sproing" instability [29]. It results from a gradient-induced phase shift along the filament that leads to a twist along the filament. This instability has been studied experimentally by applying gradients of temperature [25,30], of illumination intensity [31], and of excitability (due to gradients in the CO_2 concentration) [13,14,18–21] to the BZ medium.

Gradient fields were also found to induce the reorientation of scroll rings [25,32–34] and of sufficiently obliquely oriented scroll waves [35]. In the case of scroll rings which usually

*christian.bruns@med.ovgu.de
†marcus.hauser@ovgu.de

shrink due to their positive line tension [24], gradients may both lead to the prolongation of their lifetimes [25,34] and even revert the contraction to an expansion of the scroll ring [33].

In confined geometries, the confinement has been found to couple back on scroll waves and rings and to affect their behavior. For instance, unstable scroll rings can be stabilized by the interaction with confining boundaries, even though the line tension of the ring is negative. Under bulk conditions such scroll rings would be destabilized [36–38]. Spatial confinement may also reduce the shrinkage rate of filaments with positive line tension and alter the lifetimes of such scroll rings [39].

In the present paper we investigate the dynamics of scroll waves in a confined but still fully 3D topology, namely, in a cylinder jacket–shaped reactor. The thickness of the reaction medium is constant such that 1.50–1.66 wavelengths of the scroll wave can be hosted in the cylinder jacket. Furthermore, the medium is isotropic. Hence, the chosen geometry represents the simplest approximation to the geometry of the heart as a hollow organ. We study the dynamics and fate of scroll waves in this setting and observe that the scroll wave may (i) remain unaffected by the reactor geometry, (ii) reorient and shrink, or (iii) vanish altogether. The conditions and the kinetics leading to these three fates are investigated experimentally. In the paper we first present the experimental methods (Sec. II) followed by the experimental results (Sec. III) and, finally, we discuss our results (Sec. IV).

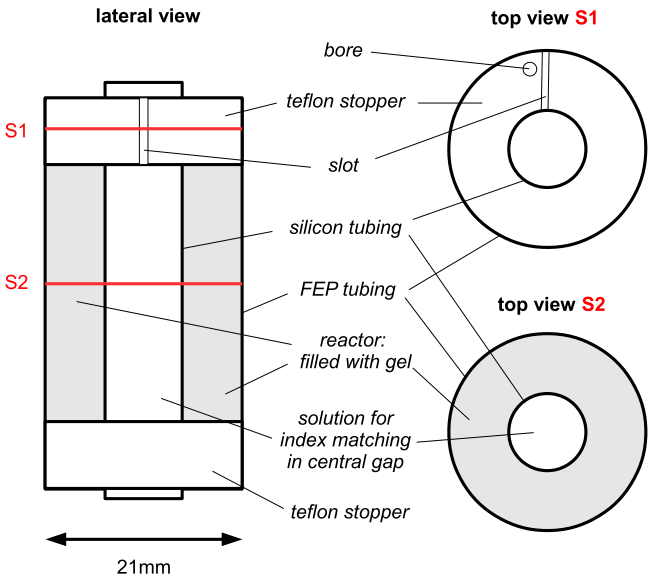

FIG. 1. Scheme of the reactor: Lateral view and two horizontal slices S1 and S2. The reaction volume is shown in grey. The central silicon tubing with an outer diameter of either 5 or 6 mm forms the central gap and is filled with a solution for index matching. The reaction volume is confined by the internal silicon tubing and the external FEP cylinder of 21 mm inner diameter. On top and bottom the reactor is sealed by two Teflon stoppers. The horizontal slice S1 shows the setting of the top stopper, which has a bore and a slot for initiating a vertical wave front. The horizontal slice S2 shows the cylinder jacket geometry of the reaction volume.

II. MATERIAL AND METHODS

Experiments were run in a cylinder jacket–shaped reactor (Fig. 1). It consisted of an outer tube made of fluorinated ethylene propylene (FEP) and an inner silicon tube that were arranged concentrically. At the top and bottom, the reactor was sealed by two Teflon stoppers. The inner diameter of the FEP tube was 21 mm and the outer diameter of the central silicon tube was either 5 or 6 mm, yielding a cylinder jacket–shaped reaction volume of uniform width of 7.0–7.5 mm. The height of the reaction medium was 21–26 mm.

We used the ferroin-catalyzed BZ reaction embedded in a 1.0% wt/vol (weight per volume) agarose (type VII, Sigma) gel matrix to suppress any hydrodynamic effects that may otherwise interfere with the wave fronts. To diminish and retard the production of CO_2 bubbles, 0.2 mM of the surfactant sodium dodecyl sulfate (SDS, Fluka) were added, i.e., at a concentration below its critical micelle concentration [18]. The initial concentrations of the BZ reactants were 50 mM malonic acid (Merck), 50 mM sodium bromate (Merck), 210 mM sulfuric acid (Fluka), and 0.5 mM ferroin, which was added when the reaction mixture reached 27 °C.

Vertical scroll waves were initiated by the partition method [13,15,18–21,40]: Once the reactant solution had cooled down to ≈26 °C, it was filled in the reaction volume given by the cylinder jacket. Subsequently a polyethylene terephthalate (PET) sheet was immersed into the reaction volume through a slot in the Teflon stopper (Fig. 1). Then a cylindrical wave was initiated by inserting a silver wire through a bore (Fig. 1) such that the wire touched the bottom of the reactor. The silver wire was withdrawn immediately after generation of the wave front. After one edge of the wave had hit the external cylinder wall the dividing PET sheet was removed. At this instant the temperature of the soft gel was ≈24 °C so that the gel healed as it cooled down to 21 °C; i.e., any gaps were closed during the gelation process. The remaining open edge of the generated reaction front curled in to form a scroll wave.

The experiments were conducted in a laboratory whose temperature was controlled by an air conditioning system and kept constant at 21 ± 1 °C. In 2D setups the used recipe yields rigidly rotating spiral waves [41].

In three dimensions we obtained rigidly rotating scroll waves whose filaments always had a positive line tension; i.e., they had the tendency to shrink. The scroll waves had a wavelength of 4.5 ± 0.2 mm. Their filaments were determined as the central area that was never visited by the wave front during one revolution of the scroll wave. The filaments had diameters of 1.5 ± 0.5 mm.

The scroll waves were monitored by optical transmission tomography. Since the tomographic principle requires projections taken from different angles, the reactor was rotated by a stepping motor. One tomographic sample consisted of 100 projections recorded at a step size of $\Delta\theta = 1.8°$, and an acquisition rate of 25 frames s^{-1}. The images were recorded by a CCD camera (Hamamatsu XC-ST70CE; 768 × 576 pixels) at 25 frames s^{-1}, digitized and stored on a computer for later image reconstruction and analysis. The spatial resolution is 0.1 mm $pixel^{-1}$.

The chosen recipe also warranted a sufficiently slow propagation of the reaction fronts so that they were nearly

stationary during the 4 s required for the acquisition of one tomographic sample [15,41]. The information on the spatial concentration distribution is contained in the grey values of the tomographic projections. The 3D reconstruction of the structure is based on the filtered back-projection of the ferriin concentration [42].

The reaction cuvette is illuminated by a blue light-emitting diode ($\lambda \approx 470$ nm; bandwidth, 50 nm). Since the reconstruction by filtered back-projection requires a parallel light beam, light was sent through a two lens system. Furthermore, FEP was chosen as the material for the outer reaction cuvette because its refractive index $n = 1.340$ [15] is very similar to that of the BZ medium ($n = 1.338 \pm 0.002$). Finally an index matching solution consisting of 0.241 M K_2SO_4 (Merck) and 0.1 mM ferroin, that has a refractive index of $n = 1.337 \pm 0.002$, was filled into the internal silicon tubing and in a square cuvette surrounding the cylindrical reactor.

The inclination angle ϕ of the filament to the horizontal was defined in Fig. 3. The filament length was measured in the original projections. To this purpose a tangent was placed along the filament and the angle ϕ to the horizontal was measured.

III. RESULTS

In our experiments, scroll waves rotate rigidly around their filaments. Although the filaments are localized and do not move, experiments are always subject to small fluctuations such that small parts of the filament may temporally deviate slightly from their "rigid" orientation. This increases the probability that a filament hits a lateral wall when the scroll wave is confined in a narrow cylinder jacket. In such cases the filament may attach to the lateral reactor wall such that it ruptures into two parts. The fate of the scroll wave and its filament depends on the geometric arrangement of the two boundaries to which the tips of the filament are pinned. The following four situations are observed.

When the two ends of the filament attach to opposite walls, the scroll wave persists. Such a persisting scroll wave may either (1) remain vertical in the cylinder, such that its filament remains parallel to the cylinder axis as well, or (2) it may reorient, i.e., it may turn and eventually align to the horizontal if its filament pins to opposite vertical walls of the cylinder. By contrast, if the filament of the scroll wave attaches either to the same wall or to adjacent walls of the reactor the filament shrinks, either (3) giving rise to a pointlike wave source or (4) disappearing completely. In the following, we describe the evolution of the filament observed for the different cases.

A. Filaments that remain vertical

The filament of the scroll wave is a small but slightly extended object. Therefore, the probability of observing scroll waves that remain parallel to the cylinder axis increases with the width of the cylinder jacket. Figure 2 shows a scroll wave whose filament remained parallel to the cylinder axis. It retains its shape and position. Such a behavior was also observed in scroll waves in bulk cylindrical reactors [18–20].

At each revolution the scroll wave emits wave fronts, which pin to the internal and external lateral walls of the reactor and travel away from their origin. When two wave fronts that traveled through the cylinder jacket in opposite directions meet at the opposite side of the reactor, they collide with each other at obtuse angles and merge. This is a behavior similar to that of colliding wave fronts in two dimensions. The merged wave front becomes more planar and propagates toward the outer wall of the reactor, where it is annihilated upon collision with the wall. It is worth noting that collisions of wave fronts in the part of the cylinder jacket lying opposite to the filament always lead to a merger of the waves. In other words, wave-front-collision-induced generation of any new filaments was never observed (Fig. 2).

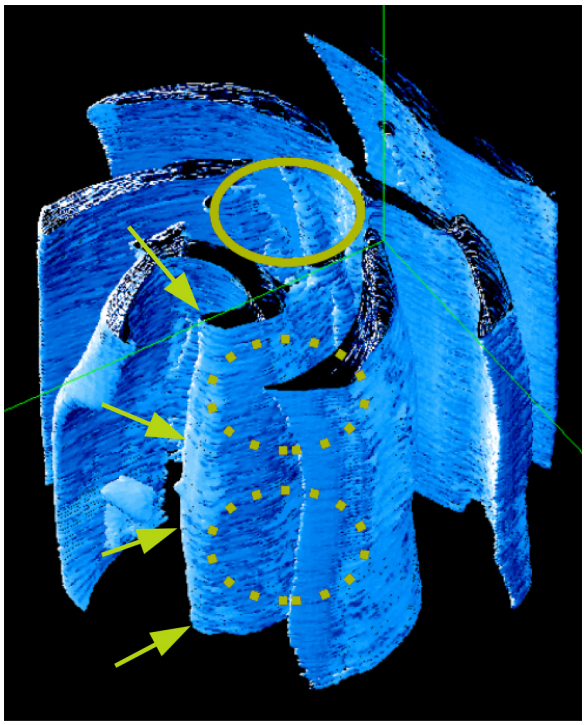

FIG. 2. Isoconcentration surfaces of the wave fronts of a vertical scroll wave in the cylinder jacket. The position of the inner tube is indicated by bright (yellow) circles. The filament of the scroll wave is located in the foreground and indicated by yellow arrows. At the side of the reactor opposite to the filament, the wave fronts are almost planar. They merge with each other, yielding almost planar fronts that propagate toward the external wall of the reactor, where they are annihilated. Sample dimensions: diameter, 21 mm; height, 15 mm.

Occasionally, the filament hit the wall, where it was annihilated, such that a traveling wave front was the only surviving structure. Such wave fronts were found to propagate around the cylinder jacket. They where annihilated by collision with another wave front propagating around the cylinder core in the opposite direction. In the lack of such a counterpart, the traveling wave front persisted until the end of the experiment.

B. Reorienting filaments

When a filament hits opposite sidewalls of the reactor, its ends adhere to these sidewalls. This generally occurs in the first 30 min after initiation of the scroll wave. The positive line tension of the filament connecting to the opposite lateral walls leads to a shortening of the filament and to its reorientation.

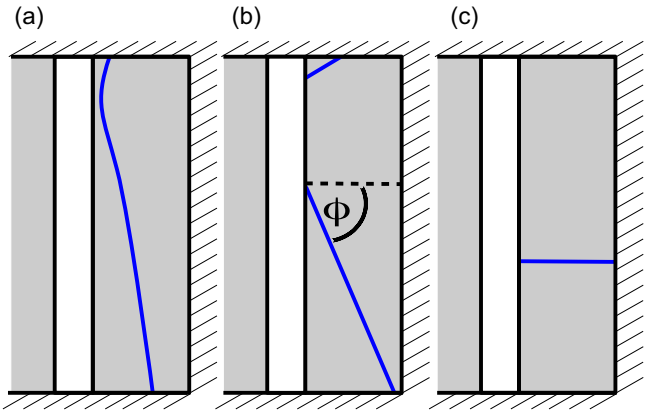

FIG. 3. Scheme of a reorienting filament over a timeline from (a) to (c). The right part of a vertical cut through the cylinder jacket reactor is shown. The reaction volume is shown in grey, the central gap of the cylinder in white, and the filament in black (blue). The inclination angle ϕ is defined as the angle between the filament and the horizontal. (a) An originally vertical filament that drifts towards the inner cylinder until it (b) hits the wall. After the collision it ruptures and the two new ends of the filaments attach to the wall. The upper filament shrunk until it disappeared as described in Sec. III C. The remaining filament shortened as well, but attached to the opposite vertical wall of the cylinder jacket. Subsequently the filament reoriented and shrunk until (c) it reached its shortest possible length.

In fact, we observed that the originally vertical filament reoriented toward the horizontal as illustrated schematically in Fig. 3. In its final position the filament aligned exactly perpendicularly to the cylinder axis [Fig. 4(a)] and spanned the shortest distance between the two parallel walls of the

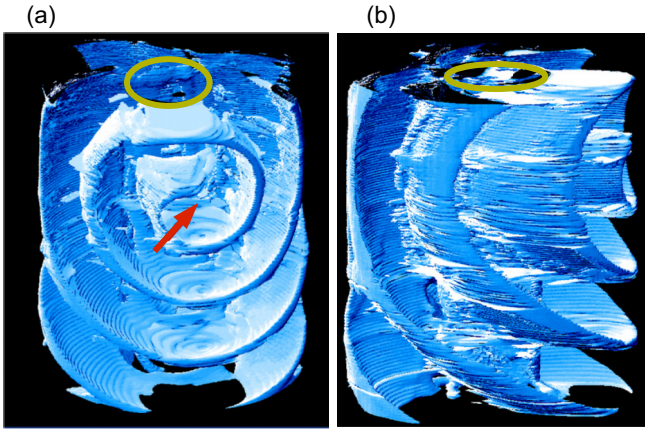

FIG. 4. Isoconcentration surfaces of the wave fronts of a horizontally oriented scroll wave. This is the final orientation of a scroll wave that attaches to two opposite lateral walls of the cylinder jacket. The orientation of the inner tube is indicated by the bright (yellow) circle. The filament is indicated by a dark (red) arrow. (a) Frontal view of the horizontal scroll wave. (b) Lateral view. The scroll wave (filament) is localized at the right-hand side of the reactor. At the side of the reactor opposite to the filament, the wave fronts emitted by the scroll wave become hemispherical, and merge with each other. There, they do not generate any new filaments. Sample dimensions: diameter, 21 mm; height, 26 mm.

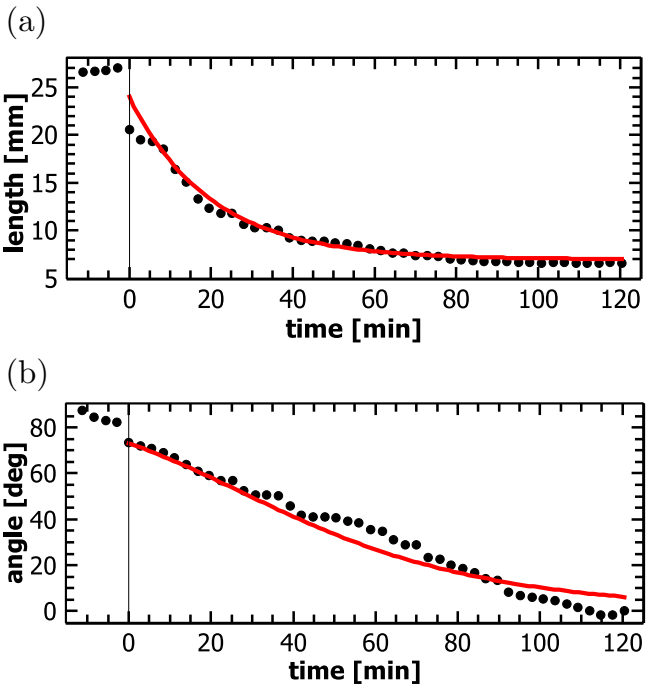

FIG. 5. Evolution of a filament after hitting two opposite lateral walls of the cylinder jacket as illustrated in Fig. 3. Time $t = 0$ defines the instant when the filament hit the two opposite walls. (a) Evolution of the filament length (dots) and a fit of Eq. (1) (line) to the measured data. (b) Behavior of the inclination angle ϕ (dots) and the fit of Eq. (2) (line) to the data. In both fits, $l_\infty = 7.0$ mm, $l_0 = 25.0$ mm, and $k = 0.05$ min^{-1}.

cylinder jacket. The horizontal filament was stable in position and shape.

The vertical position z_∞ of the horizontal filament lies halfway between the vertical positions (heights) of the two ends of the initial filament that attaches to the two opposite lateral walls of the cylinder jacket–shaped reactor, i.e., $z_\infty = 0.5(z_{0,i} + z_{0,e})$, where $z_{0,i}$ and $z_{0,e}$ are the heights where the filament was originally attached at the inner and outer walls, respectively, of the cylinder jacket.

As the filament turned from its originally vertical to the horizontal orientation, its length l decreased exponentially with time t [Fig. 5(a)] until it reached its final length l_∞. The kinetics of reorientation is described by the exponential shortening of the filament length l,

$$l(t) = l_\infty + (l_0 - l_\infty)\exp(-kt), \tag{1}$$

where l_0 is the length of the filament immediately after it had attached to the two opposite lateral walls of the cylinder jacket; k is the rate constant of the reorientation, which was found to be $k = (0.05 \pm 0.005)$ min^{-1}. The temporal evolution of the inclination angle ϕ (as defined in Fig. 3) that accounts for the orientation of the filament was found to follow the expression

$$\phi(t) = \arccos\left[\frac{l_\infty}{l(t)}\right] \tag{2}$$

to a good agreement, as shown in Fig. 5(b).

The behavior of the wave fronts emitted by the scroll wave at the reactor side opposite to the scroll wave is monitored

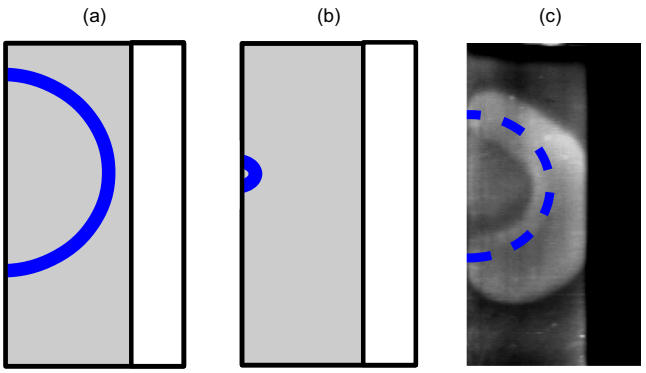

FIG. 6. Scheme of a semicircular filament. The reaction volume is shown in grey and the central gap in white. A filament [dark (blue)] with (a) both ends attached to the same wall shrinks with time to (b) a nearly pointlike wave source. (c) A single tomographic projection of the scroll wave. The filament is indicated by a dashed dark (blue) semicircle and its length is measured from this projection.

from a tomographic reconstruction done at a different axial angle of view [Fig. 4(b)]. The horizontal scroll wave emits wave fronts which propagate through the reactor. The farther the waves propagate away from the source (i.e., the filament), the more hemispherical these waves become [Fig. 4(b)]. When they reach the opposite side of the cylinder jacket–shaped reactor, they collide with each other at obtuse angles and merge. Then, they travel toward the outer wall of the reactor where they eventually annihilate. Again, no new filaments were generated by these collisions of excitable waves. This behavior is similar to that observed for vertically oriented scroll waves, as described in Sec. III A.

C. Vanishing filaments

A scroll wave vanishes if its filament either hits one lateral wall while the other end of the filament remains attached to the top or bottom of the reactor, or if both ends of the filament attach to the same wall. In both situations, the filament of the scroll wave can shorten, since the points of adhesion to the wall(s) can move towards each other.

A typical sketch and a lateral tomographic projection of a filament whose two ends are attached to the same lateral wall is depicted in Fig. 6. The corresponding scroll wave behaves as if it were a part of a scroll ring, whose positive line tension causes the filament to shrink. Such filaments shrink either to a point, yielding a pointlike wave source, or vanish altogether.

Whereas the emergence of pointlike wave sources (i.e., pacemakers) occurs due to the pinning of the shrunk, pointlike filament to any tiny defect (e.g., small scratches or imperfections of the cylinder wall) could not be determined at the resolution of our tomographic setup (of 0.1 mm pixel^{-1}).

The length of a shrinking filament was monitored from individual tomographic projections (Fig. 7) and it was also found to decay exponentially with time. This decay can also be described by Eq. (1); i.e., it followed the same kinetics as the reorienting filaments (Sec. III B). The rate constant of filament shrinkage was found to be $k = (0.04 \pm 0.02)$ min^{-1}. It is noteworthy that the values of the rate constant of filament

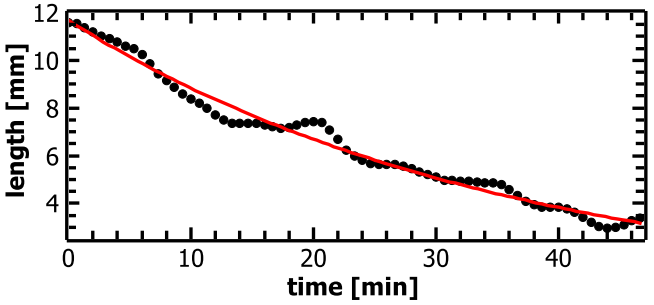

FIG. 7. Evolution of the length of the filament of a scroll wave whose ends are attached to the same wall of the cylinder jacket. Evolution of the filament length (dots) and a fit of Eq. (1) (line) to the data, with $l_\infty = 0$ mm, $l_0 = 11.6$ mm, and $k = 0.028$ min^{-1}.

shrinkage are in good agreement with that obtained for the rate constant for the filament reorientation (Sec. III B).

The relatively large error obtained for the shrinkage rate constant of shrinkage is due to manual tracking of the filaments from individual projections (rather than from any reconstructed 3D image).

IV. DISCUSSION

The dynamics of scroll waves and the orientation of their filaments in a cylinder jacket–shaped reactor were investigated. The shape of the reactor provides for both a lateral confinement of the scroll wave and for the simplest approximation of the shape of the heart as a hollow organ. The width of the cylinder jacket affected the fate of the scroll waves, as the probability that a filament hits a lateral wall of the reactor increases the narrower the cylinder jacket becomes. These tighter geometric confinements imposed by a narrow cylinder jacket favor the collision of the filament with the lateral wall.

Generally, scroll waves whose filaments were located in the middle of the cylinder jacket were persistent in shape and orientation. This corresponds to the known behavior of scroll waves in a 3D bulk cylinder-shaped reactor. By contrast, when the filament is initiated closer to a lateral wall, the probability that it hits such a wall increases. The fate of the scroll wave depends on the exact geometry of the walls to which the ends of the filaments attach: The scroll waves may either vanish or reorient.

Scroll waves reoriented when their filaments were pinned to opposite lateral walls. In the context of cardiac dynamics, such a reorientation would correspond to a transition from an originally intramural to a transmural filament.

The reorientation is associated with the shortening of the filament due to its positive line tension. The length of the filament decreases exponentially until the filament reaches its shortest possible length given by the width of the cylinder jacket. The shrinkage of vanishing filaments also follows the same exponential shrinking kinetics. In fact the shrinkage rates are similar in both cases, thus suggesting that the reorientation of the filament is governed by the dynamics of its shrinkage.

It is worth noticing that a logarithmic shrinkage of the filament of scroll waves has been observed in one of the papers introducing the line tension of the filaments of scroll waves [24]. In these simulations of filaments with a positive line

tension, it was observed that the filament of a scroll wave that is pinned to opposite sides of the reaction volume follows an exponential kinetics (Fig. 6(b) of Ref. [24]), as also seen in the present study. Reasonable agreement is also observed with the simulations of a filament that is attached to adjacent walls of the reaction container. As also observed in our experiments, the filament shrinks exponentially with time (Fig. 6(a) of Ref. [24]) until it settles at the edge of the cubic reaction volume. Once this happens, the simulations predict an enhanced shrinkage which no longer follows an exponential rate.

Another important observation is that neither new filaments nor new scroll waves are generated once the traveling waves emitted by a scroll wave collide with each other at the wake of the inner cylinder. This finding is independent of the orientation of the scroll waves with respect to the cylinder axis. Translated to the situation of cardiac tissues, this would mean that we observed neither the generation of any new filament nor any reentrance. However, we emphasize that the scroll wave dynamics studied here was always started in a reactor whose cylinder jacket had a constant width that could accommodate $\approx$1.5 wavelengths of the scroll. Apparently, this geometry is sufficiently gentle to provide for a smooth merger of colliding excitation waves in the wake of the central cylinder.

Our observations do not preclude that the generation of new filaments might be possible under somewhat different conditions, either at a different excitability of the medium (due to different BZ recipes) or by geometrical conditions, as for instance a narrower or a nonuniform width of the cylinder jacket. Studies in a cylinder jacket–shaped reactor with nonuniform width should be addressed in the near future.

ACKNOWLEDGMENT

We would like to thank Dr. E. M. Cherry (Rochester Institute of Technology) and Dr. F. H. Fenton (Georgia Institute of Technology) for fruitful and incentivizing discussions. Internal funding by the Otto von Guericke Universität is acknowledged.

[1] A. T. Winfree, Science **266**, 1003 (1994).
[2] F. H. Fenton, E. M. Cherry, H. M. Hastings, and S. J. Evans, Chaos **12**, 852 (2002).
[3] J. Xu, S. N. Menon, R. Singh, N. B. Garnier, S. Sinha, and A. Pumir, PLoS ONE **10**, e0118443 (2015).
[4] M. A. Dahlem and N. Hadjikhani, PLoS ONE **4**, e5007 (2009).
[5] N. Hadjikhani, M. S. del Rio, O. Wu, D. Schwartz, D. Bakker, B. Fischl, K. K. Kwong, F. M. Cutrer, B. R. Rosen, R. B. Tootell, A. G. Sorensen, and M. A. Moskowitz, Proc. Natl. Acad. Sci. USA **98**, 4687 (2001).
[6] M. Gerhardt, M. Ecke, M. Walz, A. Stengl, C. Beta, and G. Gerisch, J. Cell. Sci. **127**, 4507 (2014).
[7] R. A. Gray, J. Jalife, A. V. Panfilov, W. T. Baxter, C. Cabo, J. M. Davidenko, and A. M. Pertsov, Science **270**, 1222 (1995).
[8] R. A. Gray, A. M. Pertsov, and J. Jalife, Nature (London) **392**, 75 (1998).
[9] F. Fenton and A. Karma, Chaos **8**, 879 (1998).
[10] R. H. Clayton, E. A. Zhuchkova, and A. V. Panfilov, Prog. Biophys. Mol. Biol. **90**, 378 (2006).
[11] E. M. Cherry and F. H. Fenton, New J. Phys. **10**, 125016 (2008).
[12] A. T. Winfree, S. Caudle, G. Chen, P. McGuire, and Z. Szilagyi, Chaos **6**, 617 (1996).
[13] U. Storb, C. R. Neto, M. Bär, and S. C. Müller, Phys. Chem. Chem. Phys. **5**, 2344 (2003).
[14] C. Zhang, H. Liao, and Q. Ouyang, J. Phys. Chem. B **110**, 7508 (2006).
[15] C. Luengviriya, U. Storb, G. Lindner, S. C. Müller, M. Bär, and M. J. B. Hauser, Phys. Rev. Lett. **100**, 148302 (2008).
[16] T. Bánsági and O. Steinbock, Chaos **18**, 026102 (2008).
[17] T. Bánsági, K. J. Meyer, and O. Steinbock, J. Chem. Phys. **128**, 094503 (2008).
[18] D. Kupitz, S. Alonso, M. Bär, and M. J. B. Hauser, Phys. Rev. E **84**, 056210 (2011).
[19] D. Kupitz and M. J. B. Hauser, Phys. Rev. E **86**, 066208 (2012).
[20] D. Kupitz and M. J. B. Hauser, J. Phys. Chem. A **117**, 12711 (2013).
[21] P. Dähmlow, S. Alonso, M. Bär, and M. J. B. Hauser, Phys. Rev. Lett. **110**, 234102 (2013).
[22] A. T. Winfree, Science **181**, 937 (1973).
[23] A. T. Winfree, *The Geometry of Biological Time* (Springer, New York, 2001).
[24] V. N. Biktashev, A. V. Holden, and H. Zhang, Philos. Trans. R. Soc. A **347**, 611 (1994).
[25] M. Vinson, S. Mironov, S. Mulvey, and A. Pertsov, Nature (London) **386**, 477 (1997).
[26] S. Alonso, F. Sagués, and A. S. Mikhailov, Science **299**, 1722 (2003).
[27] H. Henry and V. Hakim, Phys. Rev. Lett. **85**, 5328 (2000).
[28] H. Henry and V. Hakim, Phys. Rev. E **65**, 046235 (2002).
[29] C. Henze, E. Lugosi, and A. T. Winfree, Can. J. Phys. **68**, 683 (1990).
[30] S. Mironov, M. Vinson, S. Mulvey, and A. Pertsov, J. Phys. Chem. **100**, 1975 (1996).
[31] T. Amemiya, P. Kettunen, S. Kadar, T. Yamaguchi, and K. Showalter, Chaos **8**, 872 (1998).
[32] M. Vinson and A. Pertsov, Phys. Rev. E **59**, 2764 (1999).
[33] C. Luengviriya, S. C. Müller, and M. J. B. Hauser, Phys. Rev. E **77**, 015201 (2008).
[34] C. Luengviriya and M. J. B. Hauser, Phys. Rev. E **77**, 056214 (2008).
[35] P. Dähmlow and M. J. B. Hauser, Phys. Rev. E **88**, 062923 (2013).
[36] H. Dierckx, H. Verschelde, O. Selsil, and V. N. Biktashev, Phys. Rev. Lett. **109**, 174102 (2012).
[37] A. Azhand, J. F. Totz, and H. Engel, Europhys. Lett. **108**, 10004 (2014).
[38] P. V. Paulau, J. Löber, and H. Engel, Phys. Rev. E **88**, 062917 (2013).
[39] J. F. Totz, H. Engel, and O. Steinbock, New J. Phys. **17**, 093043 (2015).
[40] A. M. Pertsov, R. R. Aliev, and V. I. Krinsky, Nature (London) **345**, 419 (1990).
[41] C. Luengviriya, U. Storb, M. J. B. Hauser, and S. C. Müller, Phys. Chem. Chem. Phys. **8**, 1425 (2006).
[42] D. Stock and S. C. Müller, Physica D (Amsterdam, Neth.) **96**, 396 (1996).